AN EXPERIMENTAL STUDY ON AN ELECTROCHEMICAL REDUCTION OF AN OXIDE MIXTURE IN THE ADVANCED SPENT-FUEL CONDITIONING PROCESS

SANG MUN JEONG*, BYUNG HEUNG PARK, JIN-MOK HUR, CHUNG-SEOK SEO, HANSOO LEE and KI-CHAN SONG
Nuclear Fuel Cycle Development Group, Korea Atomic Energy Research Institute
P. O. Box 105, Yuseong-gu, Daejeon, 306-600, Republic of Korea
*Corresponding author. E-mail : smjeong@kaeri.re.kr

Received May 26, 2009
Accepted for Publication March 9, 2010

An electrochemical reduction of a mixture of metal oxides was conducted in a LiCl molten salt containing 3 wt% Li_2O at 650ºC. The oxide reduction was carried out by applying a current to an electrolysis cell, and the Li_2O concentration was analyzed during each run. The concentration of Li_2O in the electrolyte bulk phase gradually decreases according to Faraday's law due to a slow diffusion of the O^{2-} ions. A hindrance effect of the unreduced metal oxides was observed for the reduction of the uranium oxide. Cs, Sr, and Ba of high heat-load fission products were diffused into and accumulated in the salt phase as predicted with thermodynamic consideration.

KEYWORDS : ACP, Pyroprocessing, Electrochemical Reduction, LiCl-Li_2O Molten Salt, Diffusion

1. INTRODUCTION

It is well known that pyroprocessing technology based on molten salt electrolysis is a promising option that satisfies the requirements of cost, environmental safety, and high proliferation resistance to treat spent nuclear fuels (SFs) [1-3]. Extensive investigations on a pyroprocessing have been conducted over the past several years [4-10]. An electrochemical reduction or an electrolytic reduction of the spent oxide fuels has been developed to replace the conventional metallothermic reduction between metal oxides and lithium metal dissolved in a LiCl pool, which has some drawbacks such as the process complexity, solubility limit of the reactant and product, handling of the chemically active lithium metal, and so on [11].

An electrochemical reduction by using molten salt has been studied extensively to produce a pure metal from its metal oxide form. It has been reported that this technology is a much easier, less expensive, and more environmentally friendly process than the conventional metallurgical route [12,13]. Numerous researchers in the field of nuclear energy have applied electrochemical reduction technology to reduce oxide fuels. Experimental results with spent oxide fuel have been reported in previous publications [6,14-16]. In addition, the electrochemical reduction behaviors of UO_2 and MOX have been reported by other research groups [4,7,10]. Such research results suggest that the application of an electrochemical reduction technology to a spent oxide fuel is a promising concept for the purposes of disposal and creating a closed fuel cycle for the Generation-IV fast reactor [17].

The Korea Atomic Energy Research Institute (KAERI) has developed an Advanced Spent Fuel Conditioning Process (ACP) on the basis of pyroprocessing for the purpose of a reduction in the volume, the radiotoxicity, and the heat load of spent nuclear fuels (SFs) discharged from commercial pressurized water reactors (PWRs). The final product forms of the ACP are a metallic ingot for disposal and a pellet of waste salt. The ACP consists of several steps, including slitting, voloxidation, electrolytic reduction, smelting, a waste salt conditioning process, and so on, as shown in Figure 1. In the ACP concept, the chopped SFs, mainly composed of UO_2 pellets, are oxidized at around 500ºC under an air atmosphere in the voloxidation process, where SF pellets are pulverized into oxide powder, and volatile fission products (VFPs) such as I, Kr, and Xe are removed at the same time [9]. The oxide powder is transported to an electrolytic process to be loaded into a porous magnesia basket, which is used as a cathode. The oxygen ions of the oxide powder are removed electrochemically at the cathode and, consequently, are released as oxygen gas at the platinum anodes in a LiCl salt containing 3 wt% Li_2O. Also, the salt-soluble FPs such as Cs, Sr, and Ba in the SFs are

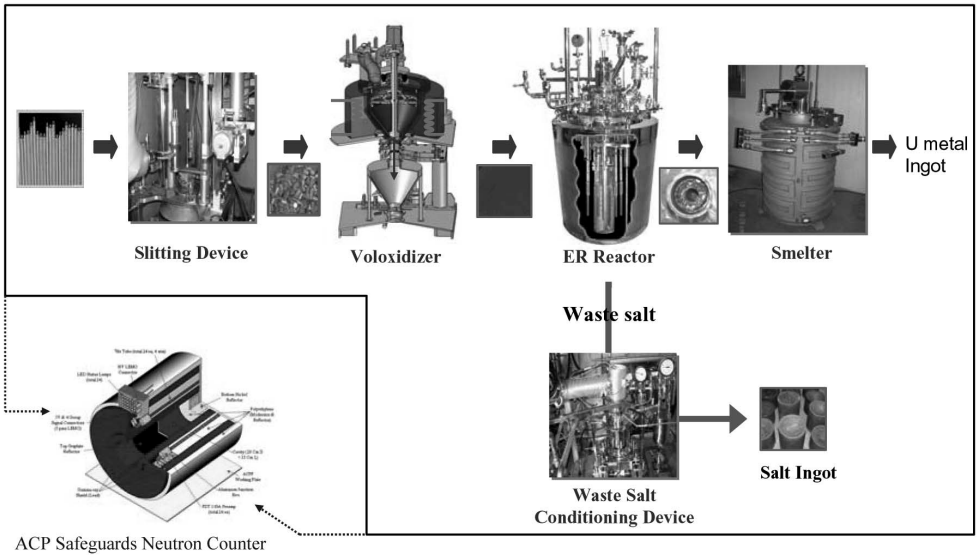

Fig. 1. Process Stream of the Advanced Spent Fuel Conditioning Process (ACP)

removed from the SFs by dissolution into the molten salt in the electrolytic reduction step. The reduced metal is sent to a smelter to remove the salt residue and to make metal ingots. The waste salt is converted into pellet form in the waste salt conditioning process and is stored and then reused in a further electrolytic reduction process.

Our research group employed an integrated cathode assembly with a porous magnesia diaphragm as a cathode basket to realize the electrochemical reduction of pure uranium oxide (U_3O_8) powder and carried out a successful scale-up study of the oxide reduction [5,11,18,19]. A previous study reported that a high reduction conversion of 99% of U_3O_8 was achieved through this system and the decomposition of Li_2O played an important role in such a high conversion [18]. Porous magnesia is also very effective to contain a fine powder of U_3O_8, which ranges from 10 to 30 μm.

In the present work, we prepared a mixture of oxide powders to simulate a voloxidized SF. The mixture powder as a surrogate of a spent oxide fuel was used as a feed material to investigate the effect of the FPs on the reduction of uranium oxide because the ACP has a voloxidation step for the pulverization of SF pellets as a head-end process for an oxide reduction process. This paper reports on the reduction characteristics of the oxide mixture, the diffusion behavior of the salt-soluble fission products, the analysis results of the metal product, and so on.

2. EXPERIMENTAL

2.1 Material

Anhydrous LiCl (99% Purity, < 20 mesh, Alfa Aesar) and Li_2O (99.5% purity, 1/4 to 100 mesh, CERAC) were used for electrolyte in this work. LiCl of 90 kg and Li_2O of 2.8 kg were fed to an electrolysis cell.

Firstly, to determine the mixture composition of the oxide powders, the composition of the spent fuel was calculated by the ORGEN code developed by the Oak Ridge National Laboratory considering the following conditions: 1) a burn-up of 43,000 MWd/tU, 2) enrichment of 3.5% U-235 and 3) a cooling period of 10 years. Then, the metal oxides such U_3O_8, alkali and alkali earth metal oxides, lanthanide oxides, and noble metal oxides were all mixed together in a ball miller on the basis of this calculation, as shown in Table 1. The physically mixed metal oxide powder of 10 kg was introduced into an electrolysis cell to conduct the electrochemical reduction.

The mean pore size and porosity of the porous magnesia diaphragm used as a cathode basket in this work were 3 μm and 22–25%, respectively. The dimensions of the basket were 150-mm i.d. × 170-mm outside diameter.

2.2 Experimental Setup

A 10 kg-batch scale electrochemical reduction system was installed at the Advanced Spent Fuel Conditioning Process Facility (ACPF). The reduction system consisted of Ar gas and reactant feeding systems, an electrolysis cell, a temperature controller, and a potentiostat/galvanostat (max. current of 200 A, WonATech Company, Republic of Korea). The electrolysis cell is comprised of an Inconel-600 crucible, a cathode assembly, an anode module with 6 platinum rods (25 mm diameter), a Pt quasi-reference electrode, and a thermocouple. The cathode assembly is made of a stainless steel current collector, a metal oxide mixture, and a non-conductive porous magnesia basket. The oxide mixture was filled in between the current collector and the magnesia basket.

Table 1. Composition of an Oxide Mixture as a Feed Material

Element	Mole percent from SF (%)	Scaled mole percent (%)	Surrogate oxide	Oxide weight percent (%)
U(+Pu)	91.23	93.32	U_3O_8	95.18
Ba	0.39	0.40	BaO	0.22
Ce(+Np)	0.57	0.58	CeO_2	0.36
La(+Am+Cm)	0.34	0.34	La_2O_3	0.41
Mo	1.03	1.05	MoO_3	0.55
Sr	0.25	0.26	SrO	0.10
Cs	0.51	0.53	Cs_2O	0.54
Y	0.15	0.15	Y_2O_3	0.12
Zr	1.17	1.19	ZrO_2	0.53
Ru(+Tc)	0.89	0.91	RuO_2	0.44
Nd(+Pr+Pm+Sm)	1.23	1.26	Nd_2O_3	1.54
Total	98.7	100		100

The details of the experimental apparatus have been described elsewhere [19].

2.3 Experimental Procedure

The electrolysis cell was flushed with high purity argon gas while it was heated to the required temperature. The electrochemical reduction was carried out at 650ºC under an Ar atmosphere to remove the oxygen gas from the cell, which was produced at the anodes. A line for cooling air was installed at a flange to prevent the evolution of salt fumes from the reactor by condensation of the salt and to protect the seal materials of the flange. The mixture of oxide powders prepared beforehand and LiCl were introduced into the reactor. The reactor was heated up and maintained at 650ºC, and then Li_2O was fed into the reactor to reach a concentration of ca. 3 wt% of the total weight of the LiCl-Li_2O molten salt. After a complete dissolution of the Li_2O in LiCl molten salt, the electrolysis cell was operated by applying a desirable current with a potentiostat. During each run, the variation of the Li_2O concentration in the molten salt was checked by a titration method, which is described elsewhere [19]. When the Li_2O concentration reached the lower limit (≈ 0.5 wt%) for stable operation, a certain amount of Li_2O was additionally introduced to the electrolysis cell. After completion of the reaction, the molten salt was transported to the salt treatment system and the cathode part was separated from the electrolysis cell. Then, the reduced metallic product was taken out of the magnesia membrane. The product was sampled for quantitative and qualitative analyses. The sample was washed and dried in a vacuum oven, and it was kept in a glove box under an inert Ar atmosphere to avoid re-oxidation. The crystalline structure of the metallic product was characterized by an X-ray diffraction (XRD) method, and a quantitative analysis of each element was performed by an Induced Coupled Plasma–Atomic Emission Spectrometer (ICP-AES).

3. RESULTS AND DISCUSSION

3.1 Thermodynamic Consideration

In the KAERI process, we have employed an electrode reaction followed by a chemical reaction mechanism by using a unique cathode assembly with a porous magnesia basket [18-20]. A powder of the metal oxides is directly fed and contained in the magnesia basket and reduced electrochemically to the corresponding metal form. The metal oxides can be reduced according to the following reaction mechanism at the operating window between 2.47 and 3.46 V, which is present between the decomposition potentials of Li_2O and LiCl.

At the cathode part,

$$Li^+ + e^- \rightarrow Li \quad (1)$$

$$M_xO_y + 2ye^- \rightarrow xM + yO^{2-} \quad (2)$$

The formed Li could proceed to a further chemical reaction with the metal oxide inside the magnesia basket.

$$M_xO_y + 2yLi \rightarrow xM + yLi_2O \quad (3)$$

Li_2O produced by Reaction (3) is redissolved in the molten salt to Li^+ and O^{2-} ions, and O^{2-} ions diffuse from the cathode to the anode across the metal/metal oxide layer, the pore of the magnesia basket, and the electrolyte bulk.

Table 2. Gibbs Free Energy Change for each Oxide in the Electrolytic Reduction

Reaction	Gibbs free energy change, ΔG_r (kJ/mol)
$U_3O_8 + 16Li \rightarrow 3U + 8Li_2O$	-845.7
$UO_2 + 4Li \rightarrow U + 2Li_2O$	-26.8
$CeO_2 + 4Li \rightarrow Ce + 2Li_2O$	-53.3
$La_2O_3 + 6Li \rightarrow 2La + 3Li_2O$	103.4
$Y_2O_3 + 6Li \rightarrow 2Y + 3Li_2O$	208.1
$Nd_2O_3 + 6Li \rightarrow 2Nd + 3Li_2O$	119.1
$MoO_3 + 6Li \rightarrow Mo + 3Li_2O$	-915.6
$ZrO_2 + 4Li \rightarrow Zr + 2Li_2O$	-27.6
$RuO_2 + 4Li \rightarrow Ru + 2Li_2O$	-802.2
$Cs_2O + 2LiCl \rightarrow 2CsCl + Li_2O$	-287.6
$BaO + 2LiCl \rightarrow BaCl_2 + Li_2O$	-55.5
$SrO + 2LiCl \rightarrow SrCl_2 + Li_2O$	1.517

Table 3. Gibbs Free Energy Change and Decomposition Potentials Calculated by HSC Chemistry [21]

Reaction	Gibbs free energy change ΔG_f (kJ/mol)	Decomposition potential (V)
$U_3O_8 \rightarrow 3UO_2 + O_2$	186.0	-0.48
$UO_2 \rightarrow U + O_2$	924.7	-2.40
$MoO_3 \rightarrow Mo + 3/2O_2(g)$	511.6	-0.88
$ZrO_2 \rightarrow Zr + O_2(g)$	923.9	-2.39
$RuO_2 \rightarrow Ru + O_2(g)$	149.3	-0.038
$Li_2O \rightarrow 2Li + 1/2O_2$	475.7	-2.47
$LiCl \rightarrow Li + 1/2Cl_2$	333.7	-3.46
$CsCl \rightarrow Cs + 1/2Cl_2$	353.1	-3.66
$BaCl_2 \rightarrow Ba + Cl_2$	710.7	-3.68
$SrCl_2 \rightarrow Sr + Cl_2$	690.0	-3.58

$$Li_2O \rightarrow 2Li^+ + O^{2-} \quad (4)$$

At the anode part, oxygen gas can be discharged by an oxidation reaction of the oxygen ions.

$$O^{2-} \rightarrow 1/2O_2(g) + 2e^- \quad (5)$$

Reactions (1) and (2) could take place on the surface of the cathode at the same time.

According the above mechanism, the main chemical reaction between the metal oxides as a feed material and the electrochemically produced lithium metal is Reaction (3) although several chemical reactions are thermodynamically favorable between the metal oxides, LiCl and lithium [20]. Also, the salt-soluble elements such as Cs, Sr, and Ba may proceed with the following reaction in the LiCl-Li_2O molten salt to be dissolved into the electrolyte.

$$MxOy + 2yLiCl \rightarrow M_xCl_{2y} + yLi_2O \quad (6)$$

Table 2 summarizes the Gibbs free energy change of each oxide fed into the magnesia basket for the present electrochemical reduction [21]. According to the thermodynamic calculation, uranium oxides (U_3O_8 and UO_2) and noble metal oxides (MoO_3, ZrO_2, and RuO_2) are easily reduced by lithium metal while the reduction of lanthanide oxides (La_2O_3, Y_2O_3 and Nd_2O_3) is unfavorable. Also, alkali metal and alkaline earth metal oxides (Cs_2O, BaO, and SrO) are converted to their chlorides in the molten salt based on the Gibbs free energy change and the activity calculation reported in a previous publication [20]. Therefore, alkali and alkaline earth metals are dissolved easily in the LiCl salt and can be removed from the cathode basket after the chlorination of Reaction (6).

The calculated decomposition potentials of the oxides and chlorides, which may be involved in the electrochemical reaction, are summarized in Table 3. U_3O_8 is electrochemically reduced to be UO_2 by applying a low cell voltage. A direct electrochemical reduction of the UO_2 and novel metal oxides is also favorable, as shown in Table 3, at our operating condition (2.47–3.46 V), which allows for a selective decomposition of Li_2O to produce lithium metal without the decomposition of LiCl [18]. We have to note that alkali and alkaline earth chlorides, which could be produced by Reaction (6), are much more stable than LiCl when considering their activity in the LiCl salt. This result implies that the high heat-generating FPs of SFs such Cs, Sr, and Ba can be partitioned stably to a salt phase during an electrochemical reduction operation.

3.2 Electrochemical Reduction

Two reduction tests (125 and 140% electrical charge relative to the theoretical charge necessary for a complete reduction of the metal oxides) with the same composition of the oxide powders listed in Table 1 were carried out in this work. The chronopotentiometric technique, where the potential is measured by controlling the current, was employed to carry out the electrochemical reduction of 10 kg of a powder mixture of metal oxides. We applied the current from 40 A to 90 A stepwise and measured the cathode and anode potentials against a platinum quasi-reference electrode. Figure 2 shows a chronopotentiogram

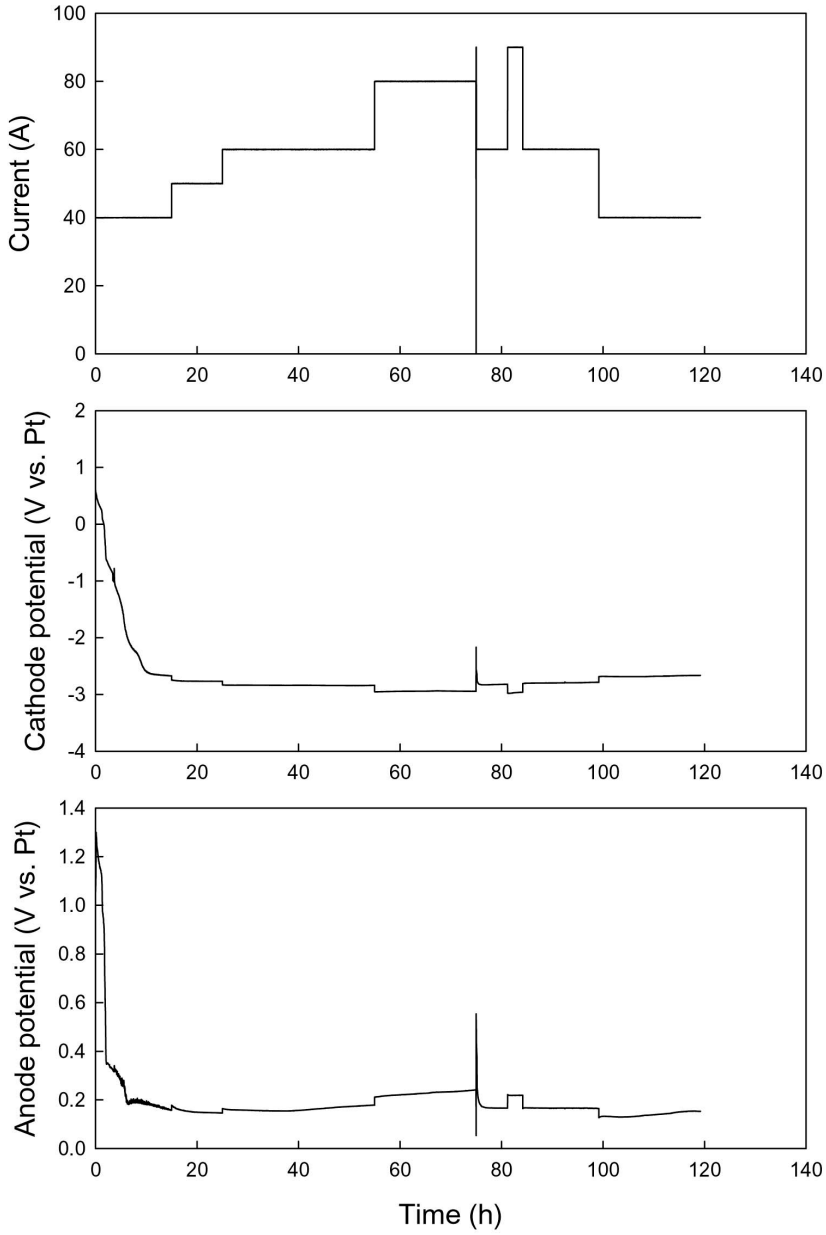

Fig. 2. Applied Current, Cathode Potential and Anode Potential Obtained in an Electrochemical Reduction of an Oxide Mixture

during the electrochemical reduction of the oxide mixture. The response potentials of the mixture are similar to that of pure U_3O_8 powder [18,19]. The cathode and anode potentials decrease sharply at the beginning of a run and then exhibit a pseudosteady state, where they vary at a narrow range of the potential. The anode potential starts to increase at a reaction time of 50 h, indicating a depletion of the O^{2-} ions around the anodes. Indeed, the concentration of Li_2O measured at the electrolyte bulk was about 1.2 wt% at the reaction time, as shown in Figure 3. As the applied current and the reaction time increase, the anode potential moves toward a more anodic direction while the cathode potential remains stable. The run was stopped to protect the Pt anode from a dissolution reaction of Pt to Pt^{2+} ions after 75 h because the Li_2O concentration reached the lower operating limit. It was reported that a higher anode potential brings about Pt dissolution as an anodic process [22]. Thus, a certain amount of Li_2O was additionally fed into the electrolysis cell, and the cell was maintained to dissolve the Li_2O for a while at 650ºC without applying a current. The current was applied again in the cell for a further reduction of the oxide mixture.

During the run, the Li_2O concentration of the electrolyte bulk was monitored as a function of the reaction time, as

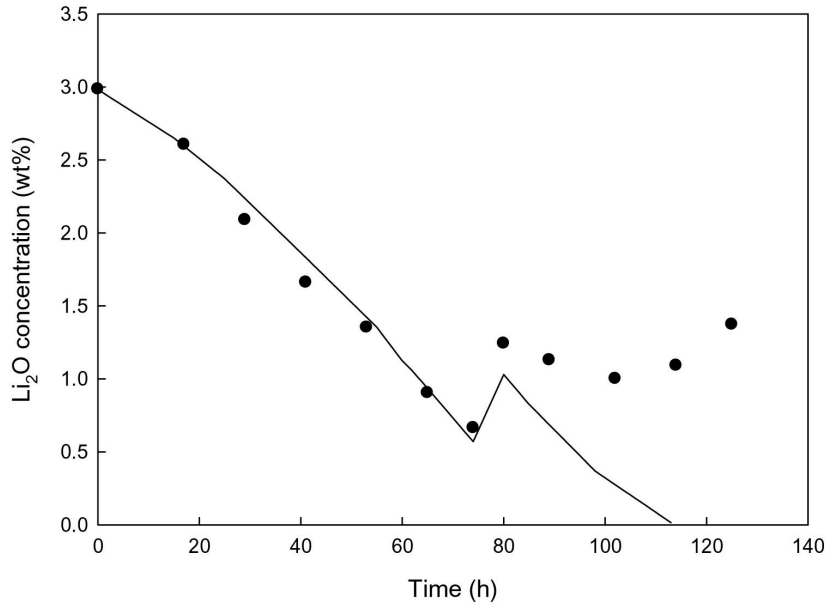

Fig. 3. Variation of Li_2O Concentration as a Function of Reaction Time. Line: Calculated Value by Faraday's Law, Symbol: Measured Value

shown in Figure 3. The concentration of Li_2O gradually decreases according to Faraday's law up to a reaction time of 75 h. This result suggests that diffusion rate of the O^{2-} ion from the cathode basket is very slow when the porous magnesia is employed as a cathode basket. At a latter part of the run (> 100 h), the Li_2O concentration increases with the reaction time because the diffusion rate of the O^{2-} ion is faster than its consumption rate. The behavior of the O^{2-} ion was reported in our previous publication [19]. As the reaction proceeds, the concentration of the O^{2-} ion inside the cathode increases gradually, while that in the electrolyte bulk decreases according to the reaction mechanism. As a result, the O^{2-} ion diffuses to the electrolyte bulk due to a concentration gradient of the O^{2-} ion between the inside and the outside of the magnesia membrane. The active O^{2-} ion diffusion probably prevents a depletion of the Li_2O in the electrolyte bulk, which brings about an increase in the anode potential. Also, it helps to decrease the reactor volume from the standpoint of a scale-up since a reduction of the oxides could be conducted even with an amount of lithium less than the stoichiometric value for Reaction (3). Moreover, a lower oxygen ion concentration in the cathode basket leads to an increase in the reduction conversion of the FPs of spent fuel. However, unfortunately, the diffusion rate of the O^{2-} ion seems to be extremely low in this work since a layer of fine powder and a relatively thick magnesia wall with a small pore size and porosity play the role of a diffusion barrier. Various attempts to accelerate the diffusion of O^{2-} ions have been made to increase the reduction rate of an oxide in terms of a scalabilty [4,23].

3.3 Behavior of Salt-soluble Elements

The diffusion behaviors of Cs, Sr, and Ba as high heat-generating FPs from a cathode basket to an electrolyte phase have been investigated during an electrochemical reduction. A small amount of salt was taken from the electrolyte bulk phase during the run to determine the concentration of each element by ICP-AES. The experimental results are shown in Figure 4, where the model described below was fitted together with experimental data obtained in this work. The concentration of those three elements increases with the reaction time by forming their chloride forms as listed in Table 2.

The dissolution of Cs_2O, BaO, and SrO into a bulk molten salt phase from the cathode basket is understood as being rate limited by diffusion. A diffusion model describing a mass transfer of a component from a cylindrical source to a bulk phase was developed in a previous work [24]. Based on Fick's diffusion equation for a long cylinder where no diffusion takes place along the axial direction, the following initial and boundary conditions are available for the current system assuming the initial concentration, C_0, was uniform inside the whole cylinder and the mass flux at the cylinder surface was equivalent to that of the liquid phase:

$$\frac{\partial C}{\partial t} = \frac{1}{r}\frac{\partial}{\partial r}\left(rD\frac{\partial C}{\partial r} \right) \tag{7}$$

$$C = C_0, \qquad \text{at} \quad 0 \le r \le a \quad \text{and} \quad t = 0 \tag{8}$$

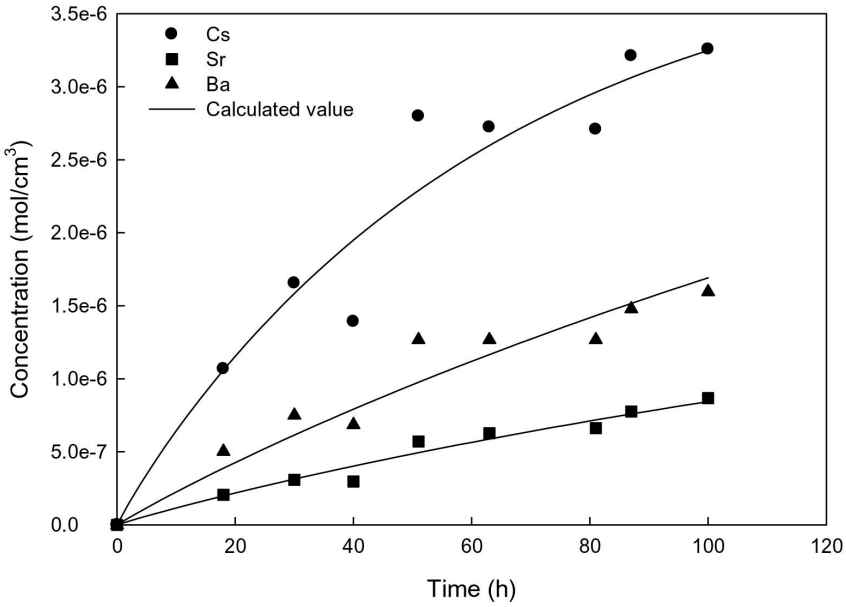

Fig. 4. Concentration Variation of Cs, Sr and Ba in the Salt Phase as a Function of Reaction Time

$$-D\frac{\partial C}{\partial r}=\alpha\left(C_s-C_e\right),\quad \text{at}\ \ r=a\ \ \text{and}\ \ t>0 \tag{9}$$

where D and α stand for the diffusion coefficient in the oxide loaded cylinder and the mass transfer coefficient at the surface of the cylinder with radius a, respectively. C_s denotes the concentration within the cylinder, and C_e is the equilibrium concentration in the bulk phase. A solution of Eq. (7) can be further arranged as a fraction of the total amount of a substance at time t, M_t, over an amount after an infinite time, M_∞, to describe the concentration changes of a concerned substance in a molten salt phase as follows [24]:

$$\frac{M_t}{M_\infty}=1-\sum_{n=1}^{\infty}\frac{4L^2\exp\left(-\beta_n^2 Dt/a^2\right)}{\beta_n^2\left(\beta_n^2+L^2\right)} \tag{10}$$

where the β_n s are the roots of the following equation including the Bessel functions of the first kind of order zero, J_0, and the first order, J_1.

$$\beta J_1(\beta)-LJ_0(\beta)=0 \tag{11}$$

A dimensionless parameter L in Eq. (11) is defined as

$$L=a\alpha/D \tag{12}$$

Eq. (10) is a working equation for correlating experimental data with the diffusion and the mass transfer coefficients for each experiment.

Table 4. Diffusion Coefficients, Mass Transfer Coefficients, and Effective Solubilities

	D [cm^2/h]	α [cm/h]	M_∞ [mol/cm^3]
Cs	2.93	0.17	4.05×10^{-6}
Sr	0.91	0.05	2.12×10^{-6}
Ba	0.75	0.04	4.86×10^{-6}

*Determined to $Min\sum_{t=1}^{NT}\left|\frac{M_t^{measured}-M_t^{calculated}}{M_t^{measured}}\right|$

When the diffusion coefficient and the mass transfer coefficient with M_∞ are known, the accumulated concentration with respect to the experimental time can be calculated by Eq. (10). In this work, they were regressed by minimizing the summation of relative deviations between measured concentrations during a run and calculated ones from Eq. (10) at each measured point.

The diffusion coefficient and the mass transfer coefficient for each metallic element are listed in Table 4. The values in Table 4 were determined by minimizing deviations between measured concentrations during a run and calculated ones from Eq. (10). As can be seen in Figure 4, the alkali and the alkaline earth metals are diffused into and accumulated in the salt phase from the oxide mixture in the cathode basket and the model equation corresponds well with the experimental data. The dissolution of Cs into the bulk molten salt was fastest among the three considered elements, which is explained by the highest diffusion coefficient and the mass transfer coefficient of

Cs. Interestingly, the regressed parameter of M_∞ for Ba exhibits the greatest value, where it is expected that Ba diffuses gradually but slowly at the initial stage due to the low values of the diffusion coefficient and the mass transfer coefficient of Ba. After a reaction time of 100 h, Cs, Sr, and Ba were partitioned to a salt phase up to 76, 80 and 99% of the initial amount of those elements loaded into the cathode basket, respectively.

3.4 Product Analysis

The magnesia basket, where 125% of the theoretical charge was passed, was taken out of the electrolysis cell to analyze the reduced sample and the salt residue inside the basket. The magnesia was cut off and removed from a mixture of the reduced metal or the unreduced metal oxide and the solidified salt. Several product samples were taken out at various positions and washed to obtain a salt-free product with distilled water. Thereafter, the samples were dried at in a vacuum oven. To measure the weight fraction of the salt inside the basket, the samples were weighed before washing and after drying. Also, the aqueous solutions used for rinsing the recovered samples were collected, and the amount of Li_2O/lithium metal as a Li_2O equivalent in the salts were determined by a titration method.

Table 5 summarizes the weight fraction of the salt in the product samples and the amount of the Li_2O equivalent in the salt removed from the recovered samples along with a sampling height at the magnesia basket. The actual salt fractions in the samples may be somewhat lower than the values in Table 5 when considering the hygroscopic property of LiCl. However, a considerable amount of the salt was contained in the reduced sample due to the void fraction of the mixture of oxide powders fed into a cathode basket. Residue lithium metal can react with water to become LiOH (Li^+ and OH- ions) by releasing hydrogen gas, while Li_2O is dissolved into LiOH in water without an evolution of hydrogen gas in a washing step. A vigorous gas formation was observed during the washing of the samples, which means a large amount of lithium metal as well as Li_2O was contained in a sample. Thus, the Li_2O and Li contents were measured as Li_2O equivalent values at the same time as shown in Table 5 because we could not recover only lithium metal from the samples. Very high concentrations of Li_2O and lithium metal were found at the middle and the bottom parts of the cathode basket. Such a high concentration may come from the unreacted lithium metal produced by the electrolysis of Li_2O (Reaction 1) and the accumulation of the O^{2-} ions released from the meal oxides in a cathode basket. As described in a previous section, the Li_2O concentration (O^{2-} ion concentration) in an electrolyte bulk phase decreases due to the slow diffusion rate of the oxygen ions during an electrolytic run, and this phenomenon probably brings about an increase in the concentration of the O^{2-} ions released from the metal oxides in a cathode basket. Interestingly, the Li_2O equivalent atop the cathode is very low compared to that in the other parts. The diffusion rate of the O^{2-} ions at the top may be relatively fast because the oxide powder does not play the role of a diffusion barrier. Also, the lithium metal produced by Reaction (1) could be vaporized to a gas phase at 650ºC due to its high vapor pressure, as reported in a previous publication [25]. The concentration of Li_2O in the middle and the bottom parts is much higher than the solubility limit of Li_2O in the LiCl molten salt at 650ºC. Therefore, a solid phase of Li_2O might appear in the cathode basket during the electrolytic run.

Table 5. Weight Fraction of Salt in the Recovered Cathode Basket and the Li_2O Equivalent (wt%) of the Salt Inside the Cathode

Sample	Weight fraction of salt	Li_2O equivalent (wt%) in the salt
Top	0.33	1.24
Middle	0.40	44.00
Bottom	0.39	51.38

The recovered powders were characterized to define their crystalline structures by an XRD. Figure 5 shows the XRD result of the powders taken from two different sampling parts, the vicinities of the current collector (a) and the magnesia wall (b), respectively. The complex peaks appear because various metal oxides were all mixed together. Therefore, it is very difficult to assign each peak, but the characteristic peaks for metallic uranium and UO_2 are the major components. We have to note that the peaks related to U_3O_8 do not appear because U_3O_8 is reduced to UO_2 by an electrochemical reduction, as shown in Table 3. Hence, UO_2, rather than U_3O_8, remains as the main uranium oxide in a cathode basket during an electrolytic run. The characteristic peak for UO_2 appears for a sample taken from around the magnesia wall regardless of the supplied charges, indicating that the reduction extent of the uranium oxide around the current collector is higher than that in the vicinity of the magnesia wall. It seems that the electrochemical reduction proceeds from the current collector to the magnesia wall. Also, the intensity of the UO_2 peak in Figure 5(A) is lower than that in Figure 5(B), which suggests that the reduction extent increases with an increase of the supplied charges. The present authors previously reported a reduction conversion higher than 99% regardless of the sample position and a high current efficiency of 90% in an electrochemical reduction of pure U_3O_8 using a 10 kg batch-scale reactor [18,19]. In this work, however, the reduction degree may decrease due to a hindrance effect of the unreduced metal oxide, mainly the lanthanide oxides, although we did not measure the reduction conversion of each oxide in the cathode basket due to the difficulties of performing a quantitative analysis on them.

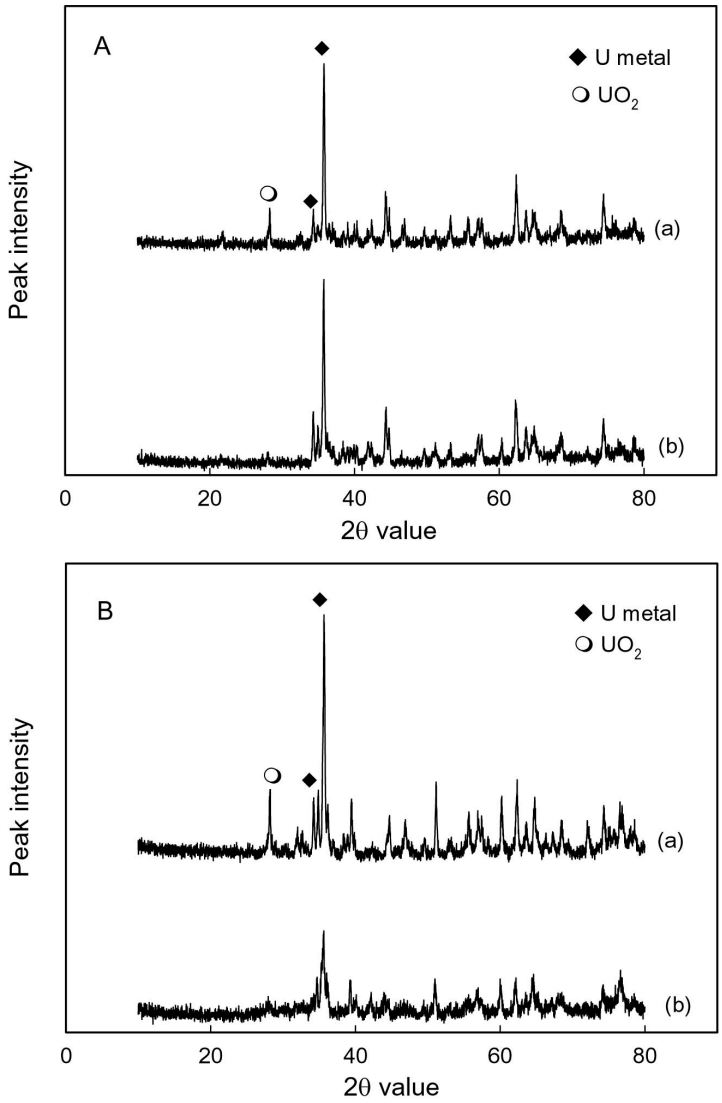

Fig. 5. X-ray Diffraction Patterns of the Reduced Samples: (A) 125 % and (B) 140 % of the Theoretical Charge. The Samples were Taken at the Vicinities of the Current Collector (a) and the Magnesia Wall (b), Respectively

4. CONCLUSIONS

An electrochemical reduction technology has been developed as a key unit process of the ACP for the efficient disposal of oxide spent fuels. In the present work, a mixture of metal oxide powders as a surrogate of a spent oxide fuel was used as a feed material to investigate the effect of the fission products on the reduction of uranium oxide and the diffusion behavior of the salt-soluble fission products. An integrated cathode assembly, which consists of a porous magnesia basket, a stainless steel current collector and the oxide powder, and a platinum anode module were employed to carry out an electrochemical reduction in LiCl molten salt containing 3 wt% Li_2O. Uranium oxide was successfully reduced at 650ºC, but the reduction degree and the current efficiency decreased due to the hindrance effect of the unreduced metal oxide compared to those in the electrochemical reduction of pure U_3O_8. The alkali and alkaline earth metals such as Cs, Sr, and Ba were diffused into and accumulated in the salt phase from the oxide mixture in the cathode basket as predicted with thermodynamic consideration. However, the diffusion rate of the oxygen ions, which has a strong effect on the scale-up and the reduction conversion of FPs, were very slow when porous magnesia was used as a cathode basket.

ACKNOWLEDGEMENT

This research was carried out under the Nuclear R&D Program supported by the Ministry of Science and

Technology, Republic of Korea. The authors would like to express their gratitude for a grant-in-aid from the Ministry of Science and Technology, Republic of Korea.

REFERENCES

[1] J.J. Laidler, J.E. Battles, W.E. Miller, J.P. Ackerman, E.L. Clarls, "Development of Pyroprocessing Technology," *Prog. Nucl. Energy*, **31**, 131 (1997).
[2] K.M. Goff, Treatment of Spent Nuclear Fuel with Molten Salt, 2008 Joint Symposium on Molten Salts, Kobe, Japan, 2008.
[3] R.W. Benedict, H.F. McFarlane, "EBR-II Spent Fuel Treatment Demonstration Project Status," *Radwaste Magazine*, **5**, 23 (1998).
[4] Y. Sakamura, T. Omori, T. Inoue, "Application of Electrochemical Reduction to Produce Metal Fuel Material from Actinide Oxides," *Nucl. Technol*., **162**, 169 (2008).
[5] S.B. Park, B.H. Park, S.M. Jeong, J.M. Hur, C.-S. Seo, S.-H. Choi, S.W. Park, "Charateristics of an Integrated Cathode Assembly for the Electrolytic Reduction of Uranium Oxide in a LiCl-Li_2O Molten Salt," *J. Radioanal. Nucl. Chem*., **268**, 389 (2006).
[6] S.D. Herrmann, S.X. Li, M.F. Simpson, S. Phongikaroon, "Electrolytic Reduction of Spent Nuclear Oxide Fuel as Part of an Integral Process to Separate and Recover Actinides from Fission Products," *Sep. Sci. Technol*., **41**, 1965 (2006).
[7] M. Iizuka, Y. Sakamura, T. Inoue, "Development of Pyroprocessing and Its Future Direction," *Nucl. Eng. Technol*., **40**, 183 (2008).
[8] M.F. Simpson, S.D. Herrmann, "Modeling the Pyrochemical Reduction of Spent UO_2 Fuel in a Pilot-Scale Reactor," *Nucl. Technol*., **162**, 179 (2008).
[9] J.-H. Yoo, C.-S. Seo, E.-H. Kim, H.-S. Lee, "Chemical Behavior of Fission Products in the Petrochemical Process," *Nucl. Eng. Technol*., **40**, 581 (2008).
[10] K. L. Gourishankar, L. Redey, M. Williamson, "Electrochemical Reduction of **Metal** Oxides in. Molten Salts," *Light Metals*, 1075 (2002).
[11] J.-M. Hur, C.-S. Seo, S.-S. Hong, D.-S. Kang, S.-W. Park, "Metallization of U_3O_8 via Catalytic Electrochemical Reduction with Li_2O in LiCl Molten Salt," *React. Kinet. Catal. Lett*., **80**, 217 (2003).
[12] G.Z. Chen, D.J. Fray, T.W. Farthing, "Direct Electrochemical Reduction of Titanium Dioxide to Titanium in Molten Calcium Chloride," *Nature* **407**, 361 (2000).
[13] Q. Xu, L.-Q. Deng, Y. Wu, T. Ma, "A Study of Cathode Improvement for Electro-Deoxidation of Nb_2O_5 in a eutectic $CaCl_2$-NaCl Melt at 1073 K," *J. Alloys Compounds* **396**, 288 (2005).
[14] S.X. Li, S.D. Herrmann, M.F. Simpson, D.R. Wahlquist, "Electrochemical Reduction of Uranium Oxide Fuel in a Molten LiCl/Li_2O Systems," Global 2003, New Orleans, LA, U.S. 2003.
[15] S.D. Herrmann, S.X. Li, M.F. Simpson, "Electrolytic Reduction of Spent Oxide Fuel – Bench-Scale Test Results," Global 2005, Tsukuba, Japan, 2005.
[16] S.D. Herrmann, S.X. Li, B.R. Westphal, "Electrolytic Reduction of Fast Reactor MOX Fuel at Bench Scale," 2008 International Pyroprocessing Research Conference, Jeju, Korea, 2008.
[17] H. Ohta, T. Inoue, Y. Sakamura, K. Kinoshita, "Pyroprocessing of Light Water Reactor Spent Fuels Based on an Electrochemical Reduction Technology," *Nucl. Technol*., **150**, 153 (2005).
[18] S.M. Jeong, S.-B. Park, S.-S. Hong, C.-S. Seo, S.-W. Park, "Electrolytic Production of Metallic Uranium from U_3O_8 in a 20 kg-Batch Scale Reactor," *J. Radioanal. Nucl. Chem*., **268**, 349 (2006).
[19] S.M. Jeong, J.M. Hur, S.S. Hong, D.S. Kang, M.S. Choung, C.S. Seo, J.S. Yoon, S.W. Park, "An Electrochemical Reduction of Uranium Oxide in the Advanced Spent-Fuel Conditioning Process," *Nucl. Technol*., **162**, 184 (2008).
[20] B.H. Park, S.B. Park, S.M. Jeong, C.-S. Seo, S.-W. Park, "Electrolytic Reduction of Spent Oxide Fuel in a molten LiCl-Li_2O system," *J. Radioanal. Nucl. Chem*., **270**, 575 (2006).
[21] HSC Chemistry 6.0, Outo-Kumpu Technology, Finland, 2006.
[22] Y. Sakamura, M. Kurata, and T. Inoue, "Electrochemical Reduction of UO_2 in Molten $CaCl_2$ or LiCl," *J. Electrochem. Soc*., **153**, D31 (2006).
[23] B.H. Park, H.-H. Lee, W.M. Choung, J.-M. Hur, C.-S. Seo, "Development of an Electrochemical Reduction Process in ACPF," 2008 International Pyroprocessing Research Conference, Jeju, Korea, 2008.
[24] B.H. Park, D.S. Kang, C.S. Seo, S.W. Park, "Development of a Mass Transfer Model and Its Application to the Behavior of the Cs, Sr, Ba, and Oxygen Ions in an Electrolytic Reduction Process for SF," *J. Kor. Rad. Waste Soc*., **3**, 85 (2005).
[25] J.-M. Hur, I.-K. Choi, S.-H. Cho, S.M. Jeong, C.-S. Seo, "Preparation and melting of uranium from U_3O_8," *J. Alloys Compounds* **452**, 23 (2008).